Development of antimicrobial peptide-antibiotic conjugates to improve the outer membrane permeability of antibiotics against Gram-negative bacteria

Ruka Yamauchi[a, #], Kenichi Kawano[a, #], Yousuke Yamaoka[a], Aoi Taniguchi[a], Yoshiaki Yano[a,b], Kiyosei Takasu[a], and Katsumi Matsuzaki[a, *]

a) Graduate School of Pharmaceutical Sciences, Kyoto University, 46-29 Yoshida-Shimoadachi-cho, Sakyo-ku, Kyoto 606-8501, Japan

b) School of Pharmacy and Pharmaceutical Sciences, Mukogawa Women's University, 11-68 Koshien Kyuban-cho, Nishinomiya, Hyogo 663-8179, Japan

[#] These authors equally contributed.

*) Author to whom correspondence should be addressed.

Tel.: +81-75-753-4521, Fax: +81-75-753-4578

E-mail: mkatsumi@pharm.kyoto-u.ac.jp (Katsumi Matsuzaki)

46−29 Yoshida-Shimoadachicho, Sakyo-ku, Kyoto 606-8501, Japan

Abstract: Antibiotics have been widely used in the medical field as a treatment for infectious diseases, but they are not effective against all Gram-negative bacteria because of their low permeability to the outer membrane. One of the strategies to improve the antibacterial activity of antibiotics is the coadministration of antibiotics and membrane-perturbing antimicrobial peptides for their synergistic effects. However, because of their different pharmacokinetics, their coadministration may not exert expected effects in the clinical stage. Here, we designed various antimicrobial peptide–antibiotic conjugates as a novel approach to improve the antimicrobial activity of antibiotics. Ampicillin was chosen as a model antibiotic with poor outer membrane permeability and the effects of the chemistry and position of conjugation and the choice of antimicrobial peptides were examined. One of the ampicillin conjugates exhibited significantly improved antimicrobial activity against ampicillin-resistant Gram-negative bacteria without exerting cytotoxicity against human cultured cells, demonstrating that our novel approach is an effective strategy to improve the antimicrobial activity of antibiotics with low outer membrane permeability.

Keywords: antimicrobial peptide • ampicillin • conjugate • disulfide bond • membrane permeability • Gram-negative bacterium

The emergence of multidrug-resistant bacteria is posing an urgent threat to human health. According to the list established by WHO, the pathogens of critical priority for research and development of new antibiotics (*Acinetobacter baumannii*, *Pseudomonas aeruginosa*, and *Enterobacteriaceae*) are all Gram-negative bacteria, which have two membrane systems: outer and inner membranes[1]. Antibiotics that inhibit cell-wall synthesis, such as β-lactams, or disrupt the inner membrane, such as polymyxins, must cross the outer membrane to reach their targets. Drugs that block the biosynthetic processes of proteins and nucleic acids need to permeate the inner membrane in addition to the outer membrane to bind to their intracellular objectives. Thus, the outer membrane constitutes a barrier for all antimicrobial agents, making the development of new antibiotics against Gram-negative bacteria extremely difficult. Indeed, no new class of antibiotics has been marketed for more than three decades. Furthermore, efflux systems pump out internalized drugs, causing drug resistance[2].

Antimicrobial peptides produced by living organisms including humans as a self-defense mechanism are promising candidates for a novel class of antibacterial agents because they are effective against a broad range of microorganisms, including multidrug-resistant bacteria, and the emergence of resistant bacteria is difficult[3-8]. These merits result from their general mode of action: membrane permeabilization. The polycationic and amphiphilic peptides bind to negatively charged bacterial membranes, both outer and inner, and disrupt their structures, leading to bactericidal

activity. The combined use of antimicrobial peptides and antibiotics is an attractive approach to synergize their activity and useful for the treatment of drug-resistant infections[9]. The membrane-perturbing peptides assist the drugs in reaching their targets. However, this strategy may not always work *in vivo* because of their different pharmacokinetics. Instead, the chemical conjugation of both antimicrobial agents is expected to overcome this problem. Although several attempts have been made to design peptide–antibiotic conjugates by various chemical linkages[10-20], very limited success has been achieved against Gram-negative bacteria[14, 16, 20]. It is not clear what types of peptides and linkages should be used and whether the N- or C-terminus of the peptide is better as the conjugation site. In this study, we addressed these questions using ampicillin (Amp) as a model antibiotic, the target of which, a penicillin-binding protein, is located on the periplasmic side of the inner membrane[21], and succeeded in developing a highly potent conjugate with no cytotoxicity.

Two antimicrobial peptides of different classes were used. One was the membrane-disrupting magainin analog 9P2-2 (GIKKWLHSPKKFPKKFVKKIMNS-NH_2) developed in our laboratory[22]. The other was Pro-rich oncocin (VDKPPYLPRPRPPRRIYNR-NH_2), which crosses the outer and inner membranes to reach its intracellular ribosomes without membrane lysis[23, 24]. A Cys residue was introduced either at the N- or C-terminus of the peptides. Amp was conjugated to the peptides either by a disulfide or thioether linkage. The former can be cleaved in the periplasm and cytosol[25].

Results

To synthesize peptide-Amp conjugates via cleavable (disulfide bond) and uncleavable (thioether bond) linkers in reductive environments of cells, two types of ATP derivatives, *N*-{3-(2-pyridyldithio)propanoyl}ampicillin (PDP-Amp) and Amp iodoacetate (I-Amp), were prepared (Supporting Information, Figure S1). PDP-Amp was crosslinked with the peptides bearing a cysteine residue either at the N- or C-terminus via a disulfide bond to generate Amp-SS-peptide or peptide-SS-Amp conjugates, respectively (the latter type is shown in Figure 1A). Similarly, I-Amp was conjugated with the peptides via a thioether bond to synthesize Amp-S-peptide or peptide-S-Amp conjugates (the latter type is shown in Figure 1B). The results of MS analysis and purity verification of the peptides and conjugates are listed in Supporting Information Table S1 and Figures S2–S13.

To evaluate the antibacterial activity, the minimum inhibitory concentration (MIC) values of Amp, the peptides, and conjugates against Gram-negative bacteria, *Escherichia coli* BW 25113 (*E. coli*) and *Acinetobacter baumannii* ATCC 19606 (*A. baumannii*), and a Gram-positive bacterium, *Staphylococcus epidermidis* ATCC 12228 (*S. epidermidis*), were determined at 16–20 hr after treatment using a broth dilution method[26]. Since *A. baumannii* has emerged as a multiple-drug-resistant pathogen causing nosocomial infections[27, 28], it was chosen as a model strain less susceptible to Amp. Indeed, Amp (**1**) exhibited MICs of 10, 320, and 20 μM against *E. coli*, *A.*

baumannii, and *S. epidermidis*, respectively (Table 1). The membrane-disrupting 9P2-2 peptides (**2** and **5**) were more potent than Amp. The conjugation of the antibiotic to the peptides by a S-S bond at the N (**3**) or C (**6**) terminus significantly improved antimicrobial activity against the Gram-negative bacteria, although their physical mixtures (**1** + **2**) and (**1** + **5**) did not exhibit stronger activity than **1** alone. The MICs of **3** were 1.3 and 2.5 μM, and those of **6** were 0.6–1.3 and 0.3 μM against *E. coli* and *A. baumannii*, respectively. In particular, the antibacterial activities of **3** and **6** against *A. baumannii* were significantly improved by 128- and 1067-times compared with **1**, respectively. To evaluate the synergetic effects of Amp and antimicrobial peptides we adopted the fractional inhibitory concentration index (FICI)[29]. It is defined that the combination of compounds A and B shows synergy and antagonism when FICI $\leq$ 0.5 and > 4, respectively. FICIs of conjugates were calculated similarly to the co-administration of ampicillin and peptides. Since FICIs of **3** and **6** were 0.3 and 0.1 against *A. baumannii*, respectively, these conjugates had synergistic antibacterial effects of Amp and antimicrobial peptides. FICIs of **3** and **6** were 0.4 and 0.7 against *E. coli*, respectively, meaning that a synergistic effect was observed for **3**, but not for **6**. On the other hand, no synergistic effect against *S. epidermidis* was observed for **3** or **6** based on their FICIs of 1.5 and 2.3, respectively.

To examine the role of the cleavable disulfide bond between the peptides and Amp in the synergy, the antibacterial activity was determined for the conjugates (**4**, **7**) with a thioether bond

(Table 1). The conjugates were less active than their counterparts with a disulfide bond except for **4** against *A. baumannii*, with activity equal to that of **3**. The MICs of **4** and **7** against *S. epidermidis* were not determined because the conjugation was not effective for **3** and **6**.

The oncocin peptides (**8** and **10**) were active only against Gram-negative bacteria, which have transporters for peptide internalization[4]. Neither their disulfide bond conjugates (**9**, **11**) nor mixtures of both compounds (**1** + **8**, **1** + **10**) exhibited synergistic effects. Taken together, these results demonstrate that the conjugation of Amp with low outer-membrane permeability to 9P2-2 could markedly potentiate antibacterial activity against Gram-negative bacteria even with resistance to Amp. Moreover, the cleavable disulfide bond was generally superior to the uncleavable thioether bond.

Next, the localization of conjugates in Gram-negative bacterial cells was observed by confocal microscopy. Here, BODIPY-FL maleimide was used as a surrogate of low-molecular-weight antibiotics and covalently labeled either at the N- or C-terminal Cys residue of 9P2-2 to obtain BODIPY-9P2-2 or 9P2-2-BODIPY, respectively. The final concentration of the peptides was fixed at 5 μM close to the MIC values of the peptides. The labeled peptides were mixed with the non-labeled peptides at a molar ratio of 1:4 to prevent a high background signal for precise assessment of their intracellular localization. BODIPY-9P2-2 and 9P2-2-BODIPY immediately accumulated on the bacterial surface of *A. baumannii* within several min (Figure 2). After 10 min, 9P2-2-BODIPY had

completely entered the cells (Figure 2B) while BODIPY-9P2-2 gradually translocated across the membranes (Figure 2A). Within 30 min, BODIPY-9P2-2 and 9P2-2-BODIPY entered 100% (n = 10 cells) and 98% (n = 47 cells) of cells, respectively. Similar results were obtained for *E. coli* (93% (n = 14 cells) and 71% (n = 17 cells) , respectively) (Supporting Information, Figure S14). We also examined the localization of BODIPY-oncocin and oncocin-BODIPY at 40 μM. In contrast to 9P2-2, fluorescent oncocin peptides weakly accumulated on the bacterial membrane surface of *A. baumannii* without internalization during a 30-min incubation (Supporting Information, Figure S15).

As a measure of safety, a cytotoxicity assay of the compounds against human embryonic kidney 293 (HEK293) cells at a high concentration of 100 μM was conducted (Figure 3A). Amp (**1**), Cys-9P2-2 (**2**), and the N-terminal Amp conjugate (**3**) exhibited no cytotoxicity. In contrast, the cell viability for the C-terminal Amp conjugate (**6**) was 34%, which was comparable with that of the parent 9P2-2-Cys (**5**) (Figure 3A). Similarly, the cytotoxicity of the N- and C-terminal Amp conjugates of oncocin (**9**, **11**) was not significantly different from that of the parent peptides (**8**, **10**). Therefore, these results demonstrate that the cytotoxicity of the conjugates originated from the peptides, and the introduction position of a Cys residue markedly influences the cytotoxicity. The intracellular localization of BODIPY-9P2-2 and 9P2-2-BODIPY peptides was also observed. The peptides accumulated on the plasma membrane within min (Figures 3B and C). In particular, the C-terminal BODIPY conjugate was immediately translocated into the cytosol and then induced

membrane blebbing, in accordance with the high toxicity of the parent peptide **5**. At 30 min after the peptide addition, the translocation ratio of BODIPY-9P2-2 was 3.4% (n = 175 cells) (Figure 3B), while that of 9P2-2-BODIPY was 38% (n = 292 cells) (Figure 3 C).

To elucidate the mechanism by which the difference in the Cys position can influence antibacterial activity of the peptides against the bacteria, the binding of **2** or **5** to large unilamellar vesicles (LUVs) mimicking bacterial cell membranes was examined based on a blue shift in the peak wavelength of Trp fluorescence as an indicator (Supporting Information Figure S16). LUVs were composed of 1-palmitoyl-2-oleoyl-*sn*-glycero-3-phosphocholine (POPC) / 1-palmitoyl-2-oleoyl-*sn*-glycero-3-phosphatidylglycerol (POPG) (1:1). The peak wavelength of the Trp residue was plotted against the lipid-to-peptide ratio ([L]/[P]). When the original peptide, 9P2-2 without a Cys residue, was used as a control, the binding of **2** to LUVs was weaker than 9P2-2, while that of **5** was stronger (Figure 4A). To evaluate changes in the secondary structure of 9P2-2, **2**, and **5** upon binding to LUVs, circular dichroism (CD) spectra were measured. The [L]/[P] ratio was fixed at 100, the condition in which the peptides were almost completely membrane-bound (Figure 4A). Higher [L]/[P] ratios caused low signal-to-noise ratios due to light scattering by LUVs. In the absence of LUVs, the peptides showed CD spectra reflecting random coil structures (Figure 4B). On the other hand, in the presence of LUVs, CD spectra were typical of α-helix with double minima. 9P2-2 and **2** exhibited similar α-helicity of 35% while the helicity of **5** was higher (53%). Amp

conjugation did not affect the peptide conformation because the CD spectra of **3** and **3** + LUV overlapped with those of **2** and **2** + LUV, respectively. Finally, in spite of the presence of the two helix-breaking Pro residues we compared the helical wheels of **2** and **5** using Heliquest[30] (Figure 4C), because CD spectra revealed that 9P2-2 partially forms an amphipathic helical structure upon binding to negatively charged membranes (Figure 4B). According to the Heliquest analysis, the hydrophobic moment, which is a measure of the amphiphilicity of a helix[31], was 0.537 and 0.643 for **2** and **5**, respectively, meaning that the introduction of a Cys residue into the C-terminus of 9P2-2 contributes more to the formation of an amphipathic structure compared with into the N-terminus. Moreover, the Cys residues of **2** and **5** were localized in hydrophilic and hydrophobic regions, respectively, suggesting that the Cys position in the hydrophobic region enhanced the binding affinity of the peptide to the membrane by enhancing the hydrophobic interaction between the peptide and membrane.

Discussion

By optimizing the choice of antimicrobial peptide, linker, and site of conjugation, we succeeded in developing a highly potent conjugate, **3**, which exerts strong synergetic effects against Gram-negative bacteria including the Amp-resistant *A. baumannii* (Table 1) without cytotoxicity against human cells (Figure 3). Since, in general, antibiotics and antibacterial peptides have different targets and functions for exerting their individual antibacterial activity, a cleavable linker inside bacterial cells would be desirable for optimal interaction with their targets. Indeed, the thioether conjugates (**4**, **7**) were less active in most cases (Table 1). The usefulness of a disulfide linkage was also reported for a conjugate between kanamycin and a Pro-rich peptide. However, uncleavable conjugations via an amide bond or azide-alkyne 1,3-dipolar cycloaddition (click chemistry) have been frequently utilized[10-15, 17, 18]. Although this study clearly demonstrated that the conjugation site plays a key role in the antibacterial and cytotoxic activities, the effects of the conjugation site has been hardly investigated[12]. Introduction of a Cys residue to the hydrophobic face of the amphipathic helix structure of 9P2-2 resulted in strong interaction with the membrane (Figure 4)

The compounds **3** and **6** did not exhibit synergism against *S. epidermidis* lacking the outer membrane, as judged from their FICIs (Table 1). This is due to the fact that the target enzyme of Amp is already exposed outside the cell membrane, further supporting the usefulness of membrane-perturbing peptides for the enhancement of Amp activity against Gram-negative bacteria.

In the case of oncocin, no significant reduction of MIC values was observed for **9** and **11** against any strains of bacteria (Table 1). BODIPY-oncocin and oncocin-BODIPY neither entered inside nor strongly accumulated on the surface of *E. coli* and *A. baumannii* cells at 30 min after peptide addition (Supporting Information Figure S15), while **8** and **10** at 100 μM showed slight cytotoxicity against HeLa cells (Figure 3A). In a previous paper[32], oncocin without a Cys residue exhibited MIC values of 0.5–8 μg/mL (corresponding to 0.2–3.3 μM) and 0.5–2 μg/mL (0.2–0.8 μM) against eight isolates of *E. coli* and five isolates of *A. baumannii*, respectively, while it did not show any toxic effects on HeLa cells at 600 μg/mL (251 μM). Moreover, the N-terminally 5(6)-carboxyfluorescein labeled oncocin at 30 μM was observed to accumulate on the surface at 20 min and to distribute within *E. coli* cells at 50 min. One possibility to explain the difference from our results is that introduction of a Cys residue may perturb its property of membrane permeability or ability to translocate into the cytoplasm of bacterial cells. Unlike 9P2-2 (Figure 4C), since oncocin is not a peptide that originally forms an amphipathic structure due to the Pro-rich sequence, the introduction of a Cys residue does not disturb its structure. In the present study, oncocin was found to be an unsuitable peptide to form conjugates with antibiotics while preserving its original properties.

In conclusion, by optimizing the type of antimicrobial peptides, position, and chemistry of linkage, we found that Amp-SS-9P2-2 exhibited significantly improved antimicrobial activity

against Amp-resistant *A. baumannii* without exerting cytotoxicity against HEK293 cells. The choice of nontoxic membrane-disruptive peptides and a cleavable linker would be a general strategy to develop potent antibiotic agents against emerging infectious diseases. The cost for the conjugation is much lower than that for the peptide synthesis. While the disulfide bond is stable in the extracellular space, the enantiomer may be used to avoid the degradation of the peptide by proteases. This technology would also revive candidate antibiotics that were once abandoned due to low outer membrane permeability.

Methods

Peptide synthesis

The peptides were synthesized by a standard Fmoc solid-phase synthesis method on a Rink Amide resin (0.4–0.6 mmol/g) (Thermo Fisher Scientific, MA, USA). The coupling reaction of the peptides bearing a Cys residue was done using a coupling system of 3 equivalents of amino acids with 3 equivalents of 1-[bis(dimethylamino)-methylene]-1*H*-benzotriazolium 3-oxide hexafluorophosphate (HBTU), 3 equivalents of 1-hydroxybenzotriazole (HOBt), and 6 equivalents of *N, N*-diisopropylethylamine (DIEA) at 25 ºC for 1 hr in *N,N*-dimethylformamide (DMF). The final deprotection of the peptides and cleavage from the resin were conducted using trifluoroacetic acid (TFA)/1,2-ethanedithiol (EDT)/triisopropylsilane (TIS)/water (94:2.5:1:2.5 (v/v)) for 3 hr at 25 °C. The crude peptides were purified by reverse-phase high-performance liquid chromatography (RP-HPLC) using a linear gradient from 20 to 50% acetonitrile in 0.1% aqueous TFA over 30 min (detection at 220 and 280 nm) on a COSMOSIL 5C_{18}-AR-II column (4.6 mm I.D. × 150 mm) (Nakalai Tesque, Kyoto, Japan) at 40 °C. The yields of the peptides were approximately 45–50%. The masses of the products were confirmed by a matrix-assisted laser desorption ionization time-of-flight mass spectrometer (MALDI-TOF-MS), AXIMA (Shimadzu, Kyoto, Japan), and a liquid chromatograph mass spectrometer (LC-MS), LCMS-8040 (Shimadzu). The absorbance spectrum of the peptides was measured by an Ultraviolet-Visible spectrophotometer UV-2550

(Shimadzu). The concentrations were calculated based on absorption of the tryptophan (ε = 5,690 cm^{-1} M^{-1}) or tyrosine residue (ε = 1,490 cm^{-1} M^{-1}) at 280 nm.

Synthesis of thiol group-reactive ampicillin derivates

The synthesis scheme is shown in Figure S1. To conjugate Amp with the antimicrobial peptides via a disulfide bond, *N*-3-(2-pyridyldithio)propanoyl Amp (PDP-Amp) was obtained following the previous procedure[33]. In brief, to yield (2-pyridyldithio)propionic acid (PDPA), 2,2'-dipyridyldisulfide (4.0 g, 18.4 mmol, 1.53 eq.) was dissolved into 100 mL anhydrous ethanol with 500 μL acetic acid, and then incrementally mixed with 3-mercapto-propanoic acid (1.0 mL, 12.0 mmol, 1 eq.) in 50 mL anhydrous ethanol. The mixture was stirred overnight at 25 ºC. After the solvent was removed by a rotary evaporator, silica gel column chromatography using 1:1 of hexane and ethyl acetate as the eluent yielded the compound with a yellow solid (1.6 g, 7.5 mmol, 62%). To obtain 3-(2-pyridlydithio)propionic acid *N*-succinimidyl ester (PDPS), PDPA (808.1 mg, 3.8 mmol, 1 eq.) was mixed with NHS (448.5 mg, 3.9 mmol, 1.05 eq.) and DCC (803.4 mg, 3.9 mmol, 1.05 eq.) in 13 mL anhydrous dichloromethane (DCM) and stirred for 2 hr at 0 °C on an ice bath. After the solvent was removed by a rotary evaporator, silica gel column chromatography using 1:1 of hexane and ethyl acetate as the eluent yielded the compound with a yellow solid (748.9 mg, 2.4 mmol, 64%). To obtain *N*-{3-(2-pyridyldithio)propanoyl}ampicillin (PDP-Amp) we followed the

previous procedure[34]. PDPS (748.9 mg, 2.4 mmol, 1 eq.) in 12 mL ethanol was mixed with anhydrous Amp (Nakalai Tesque) (838.6 mg, 2.4 mmol, 1 eq.) dissolved in 24 mL PBS (pH 7.4). The solution was stirred at 25 ºC for 6 hr. After the reaction, the solvent was removed by a rotary evaporator and underwent freeze-drying. The crude product was purified by RP-HPLC using a linear gradient from 30 to 40% acetonitrile in 0.1% aqueous TFA over 30 min (detection at 220 nm) on a COSMOSIL 5C_{18}-AR-II column (4.6 mm I.D. × 150 mm) at 40 °C to yield the compound with a white solid (40.2 mg, 0.08 mmol, 33%). The masses of the products were confirmed by LC-MS.

To conjugate ampicillin and peptides with a thioether bond, iodoacetated Amp (I-Amp) was prepared. Amp (10.5 mg, 0.03 mmol, 3 eq.) dissolved into 100 mL dimethyl sulfoxide (DMSO) was reacted with *N*-succinimidyl iodoacetate (2.8 mg, 0.01 mmol, 1 eq.) in 1.0 mL PBS (pH.7.4) and stirred in a dark place at 25 ºC for 2 hr. The crude product was purified by RP-HPLC using a linear gradient from 20 to 50% acetonitrile in 0.1% aqueous TFA over 30 min (detection at 220 nm and 280 nm) at 40 °C on a COSMOSIL 5C_{18}-AR-II column to yield the compound with a white solid (yield 61%).

Synthesis of Amp-peptide conjugates

To obtain Amp-SS-peptide and peptide-SS-Amp conjugates via the disulfide bond, PDP-Amp (14.0 mg, 0.025 mmol, 1 eq.) and the peptides (Cys-9P2-2, 9P2-2-Cys:114.9 mg, Cys-oncocin,

oncocin-Cys: 99.7 mg, 0.04 mmol, 1.6 eq.) were dissolved into 1 mL DMF and stirred at 25 ºC for 3 hr. To yield Amp-S-peptide and peptide-S-Amp conjugates via the thioester bond, I-Amp (1.3 mg, 0.003 mmol, 1 eq.) dissolved in 10 μL DMF was mixed with the peptides (0.003 mmol, 1 eq.) in 400 mM sodium phosphate buffer (pH 8.6, 500 μL) and stirred in a dark place at 25 ºC for 1 hr. The crude compounds were purified by RP-HPLC using a linear gradient from 20 to 50% acetonitrile in 0.1% aqueous TFA over 30 min (detection at 220 and 280 nm) at 40 °C on a COSMOSIL $5C_{18}$-AR-II column to yield the compound with a white solid. The masses of the products were confirmed by MALDI and LC-MS. The concentrations were calculated based on absorption of the tryptophan residue at 280 nm (ε = 5,690 cm^{-1} M^{-1}). The yields of Amp-SS-peptide and peptide-SS-Amp conjugates were approximately 20–30%. The yields of Amp-S-9P2-2 and 9P2-2-S-Amp conjugates were 32 and 12%, respectively.

BODIPY labeling

BODIPY FL maleimide (0.2 mg, 0.5 μmol) (Thermo Fisher Scientific) was dissolved in 10 μL DMSO, mixed with the peptides (0.4 μmol) bearing a Cys residue at either the N- or C-terminus in 100 mM sodium phosphate buffer (pH 7.5, 200 μL), and stirred at 25 ºC in a dark place for 2 hr. The BODIPY-labeled peptides were purified by RP-HPLC using a linear gradient from 20 to 40% acetonitrile in 0.1% aqueous TFA over 30 min (detection at 220 and 504 nm) at 40 °C on a

COSMOSIL 5C_{18}-AR-II column. The masses of the products were confirmed by MALDI-TOF-MS and LC-MS. The concentrations were calculated based on absorption of BODIPY at 504 nm (ε = 84,000 cm^{-1} M^{-1}). The yields of BODIPY-9P2-2 and BODIPY-9P2-2 were 12% and 10%, respectively.

MIC assay

MICs were determined by the broth dilution method[26]. Bacterial culture (the mid logarithmic phase was used) was adjusted to 5 × 10^5 CFU/mL with Muller-Hinton broth (Thermo Fisher Scientific), based on the relationship between the cell concentrations and OD_{600} (CFU/mL = OD_{600} × 3.4 × 10^8 for *E. coli* (BW 25113), OD_{600} × 3.6 × 10^8 for *A. baumannii* (ATCC 19606), and OD_{600} × 1.6 × 10^8 for *S. epidermidis* (ATCC 12228)). Bacterial suspension of 90 μL was dispensed in a 96-well plate (Corning, NY, USA), 10 μL of 10× concentrated peptide solution was added (including 0.01% acetic acid and 0.2% BSA to reduce peptide adsorption to the well). Then, the plate was incubated at 37 °C for 16–20 h depending on the growth of each bacterial strain. The OD_{600} values were measured at 595 nm on a model 680 microplate reader (Bio-Rad, Hercules, CA, USA). MIC was defined as the minimum peptide concentration that completely inhibited bacterial cell growth.

Cell culture

HEK293 cells were cultured at 37°C with 5% CO_2 in a humidified incubator. HEK293 cells were incubated in Dulbecco's modified Eagle's medium (DMEM) including 10%(v/v) fetal bovine serum (FBS), 10 units/mL penicillin G, and 10 μg/mL streptomycin.

Microscopic observation

After the culture of *A. baumannii*, the bacterial solvent was exchanged with PBS(+) by centrifugation (3000 ×***g***, 30 °C, 3 min). Bacterial suspensions of 80 μL (1×10^7 CFU/mL) were plated on a poly-D-Lys-coated glass bottom dish (Iwaki, Shizuoka, Japan) and incubated for 1 hr at 37 °C. HEK293 cells were seeded at a density of 3×10^5 cells/well on a glass base dish (Iwaki) and incubated for 48 hr before observation. Peptide solutions (labeled/unlabeled peptides = 1:4 molar ratio) were added at a final concentration of 5 μM. The images were acquired at an interval of 2–3 min on the stage at 25 ºC using a C1si confocal laser scanning microscope (Nikon, Tokyo, Japan) with a CFI Plan Apochromat VC 60× WI/1.20 objective lens. The image at t = 0 min was obtained immediately after peptide addition.

Cytotoxicity assay

The cell viability assay was performed with Cell Proliferation Reagent WST-1 (Roche, Mannheim, Germany) according to the manufacturer's protocol and our previous paper[22]. In brief,

HEK 293 cells were seeded at a density of 5×10^3 cells/well on a 96-well plate and incubated for 24 hr at 37 ºC, and then the medium were removed. The cells were treated with 100 µL/well DMEM/10%(v/v) FBS medium including Amp, the peptides, and mixtures of Amp and the peptides, or the conjugates and incubated for 24 hr at 37 ºC. After that, 10 µL WST-1 reagent was added to each well and incubated for 2–4 hr at 37 ºC. The absorbance of the medium was measured on a model 680 microplate reader with a 450–655 nm filter (Bio-Rad, CA, USA). Cell viability was determined and calculated as the following equation:

$$\text{Cell viability}(\%) = (\text{absorbance in the presence of 100 µM peptide} - \text{blank}) / (\text{absorbance in the absence of peptide} - \text{blank}) \times 100$$

Preparation of LUVs

POPC and POPG were purchased from Avanti Polar Lipids (Alabaster, AL, USA). POPC/ POPG (1:1 molar ratio) were dissolved in chloroform. The solvent was evaporated and vacuum-dried over 1 hr. A lipid membrane was hydrated with a Tris buffer (10 mM Tris, 150 mM NaCl, 1 mM EDTA, pH 7.4) and extruded 31 times through polycarbonate filters with a pore size diameter of 100 nm. The lipid concentration was determined by phosphorus analysis[35]. The diameter of LUVs (130 ± 39 nm, n = 5) was determined using Zetasizer Nano ZS (Malvern Panalytical,

Worcestershire, UK) with a scattering angle of 173° at 25 °C.

Membrane binding assay

The membrane binding of the peptides to LUVs was assessed based on a change in the peak wavelength of Trp fluorescence as an indicator. A peptide solution (4 μM) was titrated with LUVs at 30 °C and the fluorescence spectra of the Trp residue were recorded at an excitation wavelength of 280 nm on a RF-6000 fluorescence spectrophotometer (Shimadzu, Kyoto, Japan). Volume correction for dilution (up to 4%) was performed after blank spectra (LUVs alone) had been subtracted.

CD spectra

CD spectra of 20 μM peptides in the presence of LUVs at a lipid concentration of 2 mM ([L]/[P] = 100) or in the absence of LUVs in Tris buffer were obtained using a J-820 circular dichroism spectrometer (Jasco, Hachioji, Japan) at 30 °C. The samples were set in a 1-mm path length quartz cell to minimize the absorbance due to buffer components. The final spectrum was the average of the spectra scanned five times and then the difference in spectra was obtained by subtracting the blank spectra of LUV suspension at the same lipid concentration. The helicity (f_H) was calculated based on the molar ellipticity of the peptides at 222 nm using the following equation[36]:

$$f_H(\%) = ([\theta]_{222} - 2340) \,/\, (-30300) \times 100$$

Supporting Information

The Supporting Information is available at https//XXX

Contents: the synthesis scheme of thiol group-reactive Amp derivates, the purity and MS of the compounds, confocal microscopic images of *E. coli* treated with BODIPY labeled 9P2-2 peptides, confocal microscopic images of *A. baumannii* and *E. coli* treated with BODIPY labeled oncocin peptides, the peak shift of Trp fluorescence depending on the [L]/[P] ratio (PDF)

Author Information

Corresponding Author

Katsumi Matsuzaki – Graduate School of Pharmaceutical Sciences, Kyoto University, 46-29 Yoshida-Shimoadachi-cho, Sakyo-ku, Kyoto 606-8501, Japan

orcid.org/0000-0002-0182-1690

Phone: +81-75-753-4521

E-mail: mkatsumi@pharm.kyoto-u.ac.jp

Authors

Ruka Yamauchi – Graduate School of Pharmaceutical Sciences, Kyoto University, 46-29 Yoshida-Shimoadachi-cho, Sakyo-ku, Kyoto 606-8501, Japan

Kenichi Kawano – Graduate School of Pharmaceutical Sciences, Kyoto University, 46-29 Yoshida-Shimoadachi-cho, Sakyo-ku, Kyoto 606-8501, Japan

orcid.org/0000-0003-1927-2922

Yousuke Yamaoka – Graduate School of Pharmaceutical Sciences, Kyoto University, 46-29 Yoshida-Shimoadachi-cho, Sakyo-ku, Kyoto 606-8501, Japan

orcid.org/ 0000-0003-3641-8823

Aoi Taniguchi – Graduate School of Pharmaceutical Sciences, Kyoto University, 46-29 Yoshida-Shimoadachi-cho, Sakyo-ku, Kyoto 606-8501, Japan

orcid.org/0000-0003-4112-0597

Yoshiaki Yano – Graduate School of Pharmaceutical Sciences, Kyoto University, 46-29 Yoshida-Shimoadachi-cho, Sakyo-ku, Kyoto 606-8501, Japan, School of Pharmacy and Pharmaceutical Sciences, Mukogawa Women's University, 11-68 Koshien Kyuban-cho, Nishinomiya, Hyogo 663-8179, Japan

orcid.org/ 0000-0002-5557-3784

Kiyosei Takasu – Graduate School of Pharmaceutical Sciences, Kyoto University, 46-29 Yoshida-Shimoadachi-cho, Sakyo-ku, Kyoto 606-8501, Japan

orcid.org/ 0000-0002-1798-7919

Author Contributions

This study was conceived and directed by K.M. and experiment plans were made by K.M., K.K., and Y. Yano. Synthesis of compounds was carried out by R.Y. and Y. Yamaoka. Experiments and data analysis were conducted by R.Y., K.K., and A. T. The paper was written by K.K. and K.M., and revised by Y. Yano., Y. Yamaoka, and K.T. These authors, R.Y. and K.K., contributed equally to this study.

Notes

The authors declare no conflict of interest.

1) Tacconelli, E.; Carrara, E.; Savoldi, A.; Harbarth, S.; Mendelson, M.; Monnet, D. L.; Pulcini, C.; Kahlmeter, G.; Kluytmans, J.; Carmeli, Y.; Ouellette, M.; Outterson, K.; Patel, J.; Cavaleri, M.; Cox, E. M.; Houchens, C. R.; Grayson, M. L.; Hansen, P.; Singh, N.; Theuretzbacher, U.; Magrini, N.; Group, W. H. O. P. P. L. W., Discovery, research, and development of new antibiotics: the WHO priority (list of antibiotic-resistant bacteria and tuberculosis. *Lancet. Infect. Dis.* **2018,** *18* (3), 318–327.

(2) Chakradhar, S., Breaking through: How researchers are gaining entry into barricaded bacteria. *Nat. Med.* **2017,** *23* (8), 907–910.

(3) Fjell, C. D.; Hiss, J. A.; Hancock, R. E.; Schneider, G., Designing antimicrobial peptides: form follows function. *Nat. Rev. Drug Discov.* **2011,** *11* (1), 37–51.

(4) Matsuzaki, K., Antimicrobial Peptides Basics for Clinical Application. *Adv. Exp. Med. Biol.* **2019,** *70* (1), 1–9.

(5) Mookherjee, N.; Anderson, M. A.; Haagsman, H. P.; Davidson, D. J., Antimicrobial host defence peptides: functions and clinical potential. *Nat. Rev. Drug Discov.* **2020,** *19* (5), 311–332.

(6) Hoskin, D. W.; Ramamoorthy, A., Studies on anticancer activities of antimicrobial peptides. *Biochim. Biophys. Acta.* **2008,** *1778* (2), 357–375.

(7) Durr, U. H.; Sudheendra, U. S.; Ramamoorthy, A., LL-37, the only human member of the cathelicidin family of antimicrobial peptides. *Biochim. Biophys. Acta.* **2006,** *1758* (9), 1408–1425.

(8) Mohid, S. A.; Sharma, P.; Alghalayini, A.; Saini, T.; Datta, D.; Willcox, M. D. P.; Ali, H.; Raha, S.; Singha, A.; Lee, D.; Sahoo, N.; Cranfield, C. G.; Roy, S.; Bhunia, A., A rationally designed synthetic antimicrobial peptide against Pseudomonas-associated corneal keratitis: Structure-function correlation. *Biophys. Chem.* **2022,** *286*, 106802.

(9) Zhu, Y.; Hao, W.; Wang, X.; Ouyang, J.; Deng, X.; Yu, H.; Wang, Y., Antimicrobial peptides, conventional antibiotics, and their synergistic utility for the treatment of drug-resistant infections. *Med. Res. Rev.* **2022,** *42* (4), 1377–1422.

(10) Bera, S.; Zhanel, G. G.; Schweizer, F., Synthesis and antibacterial activity of amphiphilic lysine-ligated neomycin B conjugates. *Carbohydr. Res.* **2011,** *346* (5), 560–568.

(11) Arnusch, C. J.; Pieters, R. J.; Breukink, E., Enhanced membrane pore formation through high-affinity targeted antimicrobial peptides. *PLoS One* **2012,** *7* (6), e39768.

(12) Rodriguez, C. A.; Papanastasiou, E. A.; Juba, M.; Bishop, B., Covalent modification of a ten-residue cationic antimicrobial peptide with levofloxacin. *Front. Chem.* **2014,** *2*, 71.

(13) Chen, H.; Liu, C.; Chen, D.; Madrid, K.; Peng, S.; Dong, X.; Zhang, M.; Gu, Y., Bacteria-Targeting Conjugates Based on Antimicrobial Peptide for Bacteria Diagnosis and Therapy. *Mol. Pharm.* **2015,** *12* (7), 2505–2516.

(14) Mishra, N. M.; Briers, Y.; Lamberigts, C.; Steenackers, H.; Robijns, S.; Landuyt, B.; Vanderleyden, J.; Schoofs, L.; Lavigne, R.; Luyten, W.; Van der Eycken, E. V., Evaluation of the

antibacterial and antibiofilm activities of novel CRAMP-vancomycin conjugates with diverse linkers. *Org. Biomol. Chem.* **2015,** *13* (27), 7477–7486.

(15) Deshayes, S.; Xian, W.; Schmidt, N. W.; Kordbacheh, S.; Lieng, J.; Wang, J.; Zarmer, S.; Germain, S. S.; Voyen, L.; Thulin, J.; Wong, G. C.; Kasko, A. M., Designing Hybrid Antibiotic Peptide Conjugates To Cross Bacterial Membranes. *Bioconjug. Chem.* **2017,** *28* (3), 793–804.

(16) Mohamed, M. F.; Brezden, A.; Mohammad, H.; Chmielewski, J.; Seleem, M. N., Targeting biofilms and persisters of ESKAPE pathogens with P14KanS, a kanamycin peptide conjugate. *Biochim. Biophys. Acta. Gen. Subj.* **2017,** *1861* (4), 848–859.

(17) Jelinkova, P.; Splichal, Z.; Jimenez, A. M. J.; Haddad, Y.; Mazumdar, A.; Sur, V. P.; Milosavljevic, V.; Kopel, P.; Buchtelova, H.; Guran, R.; Zitka, O.; Richtera, L.; Hegerova, D.; Heger, Z.; Moulick, A.; Adam, V., Novel vancomycin-peptide conjugate as potent antibacterial agent against vancomycin-resistant Staphylococcus aureus. *Infect. Drug Resist.* **2018,** *11*, 1807–1817.

(18) Ptaszynska, N.; Olkiewicz, K.; Okonska, J.; Gucwa, K.; Legowska, A.; Gitlin-Domagalska, A.; Debowski, D.; Lica, J.; Heldt, M.; Milewski, S.; Ng, T. B.; Rolka, K., Peptide conjugates of lactoferricin analogues and antimicrobials-Design, chemical synthesis, and evaluation of antimicrobial activity and mammalian cytotoxicity. *Peptides* **2019,** *117*, 170079.

(19) Ptaszynska, N.; Gucwa, K.; Olkiewicz, K.; Legowska, A.; Okonska, J.; Ruczynski, J.; Gitlin-Domagalska, A.; Debowski, D.; Milewski, S.; Rolka, K., Antibiotic-Based Conjugates

Containing Antimicrobial HLopt2 Peptide: Design, Synthesis, Antimicrobial and Cytotoxic Activities. *ACS Chem. Biol.* **2019,** *14* (10), 2233–2242.

(20) Li, W. Y.; O'Brien-Simpson, N. M.; Holden, J. A.; Otvos, L.; Reynolds, E. C.; Separovic, F.; Hossain, M. A.; Wade, J. D., Covalent conjugation of cationic antimicrobial peptides with a beta-lactam antibiotic core. *Pept. Sci.* **2018,** *110* (3), e24059.

(21) Masi, M.; Refregiers, M.; Pos, K. M.; Pages, J. M., Mechanisms of envelope permeability and antibiotic influx and efflux in Gram-negative bacteria. *Nat. Microbiol.* **2017,** *2* (3), 17001.

(22) Azuma, E.; Choda, N.; Odaki, M.; Yano, Y.; Matsuzaki, K., Improvement of Therapeutic Index by the Combination of Enhanced Peptide Cationicity and Proline Introduction. *ACS Infect. Dis.* **2020,** *6* (8), 2271–2278.

(23) Knappe, D.; Piantavigna, S.; Hansen, A.; Mechler, A.; Binas, A.; Nolte, O.; Martin, L. L.; Hoffmann, R., Oncocin (VDKPPYLPRPRPPRRIYNR-NH2): a novel antibacterial peptide optimized against gram-negative human pathogens. *J. Med. Chem.* **2010,** *53* (14), 5240–5247.

(24) Roy, R. N.; Lomakin, I. B.; Gagnon, M. G.; Steitz, T. A., The mechanism of inhibition of protein synthesis by the proline-rich peptide oncocin. *Nat. Struct. Mol. Biol.* **2015,** *22* (6), 466–469.

(25) Ritz, D.; Beckwith, J., Roles of thiol-redox pathways in bacteria. *Annu. Rev. Microbiol.* **2001,** *55*, 21–48.

(26) Wiegand, I.; Hilpert, K.; Hancock, R. E., Agar and broth dilution methods to determine the

minimal inhibitory concentration (MIC) of antimicrobial substances. *Nat. Protoc.* **2008,** *3* (2), 163–175.

(27) Wendt, C.; Dietze, B.; Dietz, E.; Ruden, H., Survival of Acinetobacter baumannii on dry surfaces. *J. Clin. Microbiol.* **1997,** *35* (6), 1394–1397.

(28) Smolyakov, R.; Borer, A.; Riesenberg, K.; Schlaeffer, F.; Alkan, M.; Porath, A.; Rimar, D.; Almog, Y.; Gilad, J., Nosocomial multi-drug resistant Acinetobacter baumannii bloodstream infection: risk factors and outcome with ampicillin-sulbactam treatment. *J. Hosp. Infect.* **2003,** *54* (1), 32–38.

(29) Johnson, M. D.; MacDougall, C.; Ostrosky-Zeichner, L.; Perfect, J. R.; Rex, J. H., Combination antifungal therapy. *Antimicrob. Agents. Chemother.* **2004,** *48* (3), 693–715.

(30) Gautier, R.; Douguet, D.; Antonny, B.; Drin, G., HELIQUEST: a web server to screen sequences with specific alpha-helical properties. *Bioinformatics* **2008,** *24* (18), 2101–2102.

(31) Eisenberg, D.; Weiss, R. M.; Terwilliger, T. C., The helical hydrophobic moment: a measure of the amphiphilicity of a helix. *Nature* **1982,** *299* (5881), 371–374.

(32) Knappe, D.; Piantavigna, S.; Hansen, A.; Mechler, A.; Binas, A.; Nolte, O.; Martin, L. L.; Hoffmann, R., Oncocin (VDKPPYLPRPRPPRRIYNR-NH2): a novel antibacterial peptide optimized against gram-negative human pathogens. *J Med Chem* **2010,** *53* (14), 5240–5247.

(33) Horikawa, R.; Sunayama, H.; Kitayama, Y.; Takano, E.; Takeuchi, T., A Programmable Signaling Molecular Recognition Nanocavity Prepared by Molecular Imprinting and Post-Imprinting

Modifications. *Angew. Chem. Int. Ed.* **2016,** *55* (42), 13023–13027.

(34) Kannan, R. M. K., Sujatha; Romero, Roberto, Polyamidoamine (PAMAM) dendrimer-based nanodevices for use in treating neuroinflammation and imaging purposes. *World Intellectual Property Organization, WO2010147831 A1 2010-12-23*, World Intellectual Property Organization, WO2010147831 A1 2010-12-23.

(35) Bartlett, G. R., Phosphorus assay in column chromatography. *J. Biol. Chem.* **1959,** *234* (3), 466–468.

(36) Chen, Y. H.; Yang, J. T.; Martinez, H. M., Determination of the secondary structures of proteins by circular dichroism and optical rotatory dispersion. *Biochemistry* **1972,** *11* (22), 4120–4131.

Table 1 MICs and FICIs of the compounds

Compound	*E. coli* (BW 25113)		*A. baumannii* (ATCC 19606)		*S. epidermidis* (ATCC 12228)	
	MIC (μM) [a]	FICI [b]	MIC (μM)	FICI	MIC (μM)	FICI
Amp (**1**)	10.0	–	320.0	–	20.0	–
Cys-9P2-2 (**2**)	5.0	–	10.0	–	10.0	–
Amp + Cys-9P2-2 (**1** + **2**)	5.0	1.5	10.0	1.0	1.3	0.2
Amp-SS-9P2-2 (**3**)	1.3	0.4	2.5	0.3	10.0	1.5
Amp-S-9P2-2 (**4**)	2.5	0.8	2.5	0.3	N.D. [c]	–
9P2-2-Cys (**5**)	2.5	–	2.5	–	2.5	–
Amp + 9P2-2-Cys (**1** + **5**)	2.5	1.3	1.3	0.5	1.3	0.6
9P2-2-SS-Amp (**6**)	0.6–1.3	0.7	0.3	0.1	5.0	2.3
9P2-2-S-Amp (**7**)	2.5	1.3	1.3	0.5	N.D.	–
Cys-oncocin (**8**)	40.0	–	40.0	–	> 80.0	–
Amp + Cys-oncocin (**1** + **8**)	10	1.3	40	1.1	20.0	> 1.3
Amp-SS-oncocin (**9**)	5.0	0.6	> 40.0	>1.1	> 80.0	> 5.0
oncocin-Cys (**10**)	20.0	–	40.0	–	> 80.0	–
Amp + oncocin-Cys (**1** + **10**)	10.0	1.5	40.0	1.1	40.0	>2.5
oncocin-SS-Amp (**11**)	40.0	6.0	> 40.0	>1.1	> 80.0	> 5.0

a) MIC: minimum inhibitory concentration, the MIC values were determined at 16–20 hr depending on the growth of each bacterial strain after incubation with the peptides at 37 ºC. *b*) FICI: fractional inhibitory concentration index. FICI of compounds A and B as calculated using the following equation: FICI = (MIC_A in combination or conjugation / MIC_A alone) + (MIC_B in combination or conjugation / MIC_B alone)[29]. FICI equal or under 0.5 means that the two compounds have a synergic antibiological effect. *c*) N.D.: not determined.

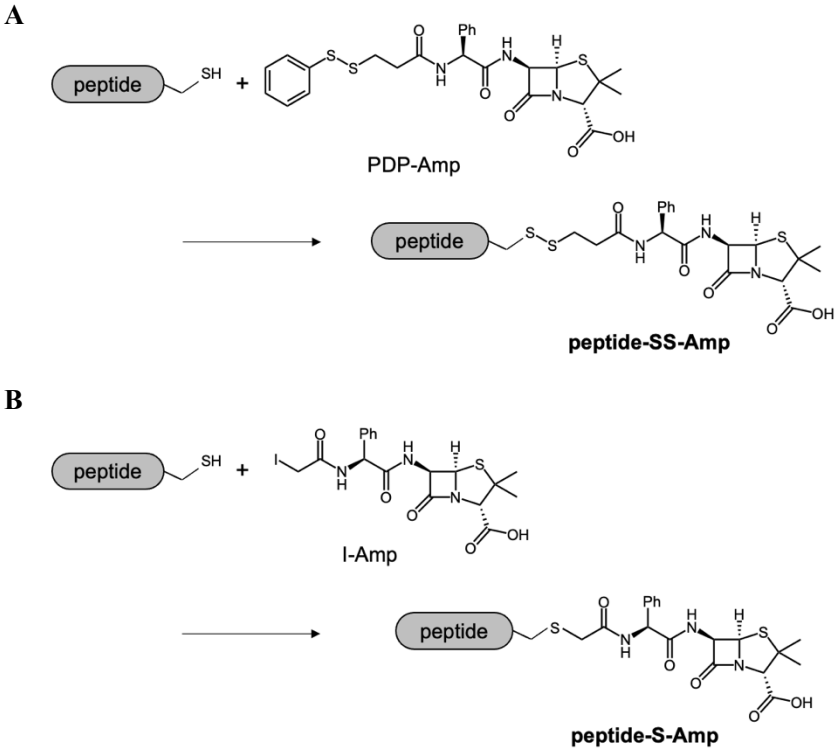

Figure 1 Synthesis scheme of the C-terminal peptide-Amp conjugates via a cleavable linker (disulfide bond) (A) and an uncleavable linker (thioether bond) (B).

A

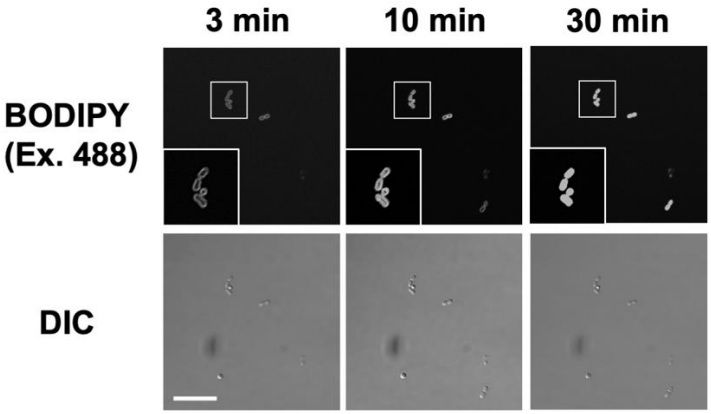

B

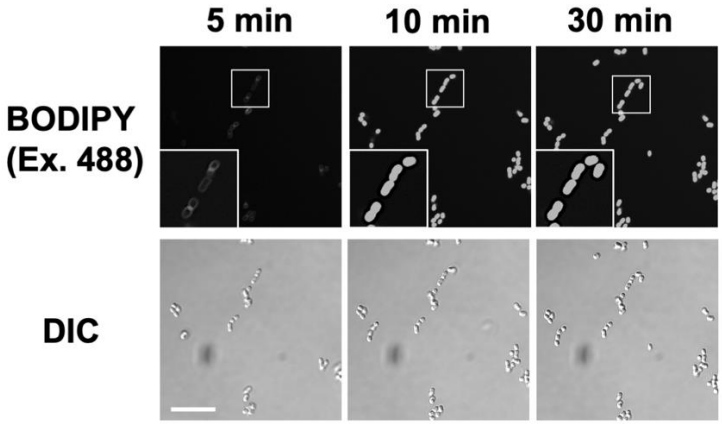

Figure 2 Confocal microscopic images of *A. baumannii* treated with (A) BODIPY-9P2-2 or (B) 9P2-2-BODIPY with each unlabeled peptide at a total concentration of 5 μM (labeled : unlabeled = 1:4 molar ratio). Upper figures are BODIPY fluorescence images excited at 488 nm and lower figures are DIC images. Scale bar, 10 μm.

Figure 3

A

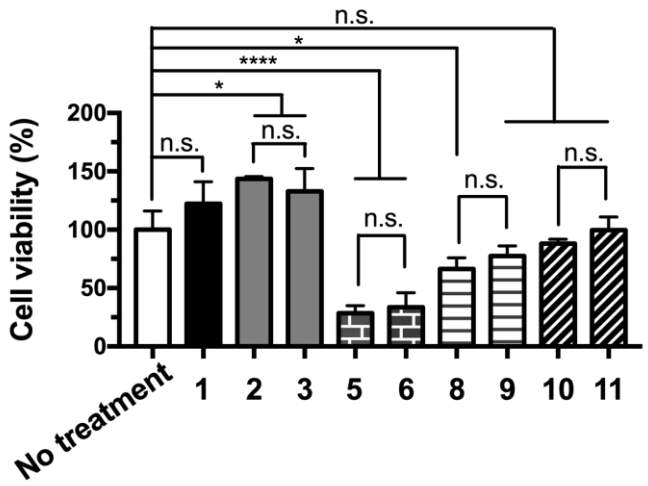
n.s.
*
****
*
n.s.
n.s.
n.s.
n.s.
n.s.
Cell viability (%)
200
150
100
50
0
No treatment
1
2
3
5
6
8
9
10
11

B

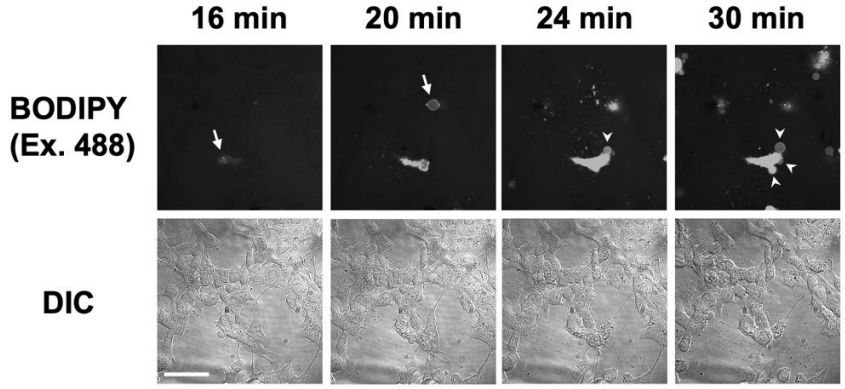
16 min
20 min
24 min
30 min
BODIPY
(Ex. 488)
DIC

C

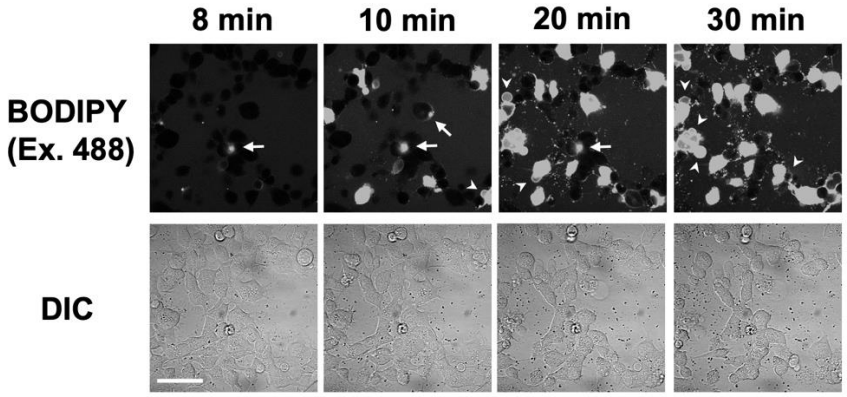
8 min
10 min
20 min
30 min
BODIPY
(Ex. 488)
DIC

Figure 3 (A) The viability of HEK293 cells treated with compounds **1**–**9** at a concentration of 100 μM for 24 hr at 37 ºC (mean ± S.D., $n = 3$). Ordinary one-way ANOVA multiple comparisons: * and **** represent $p < 0.05$ and 0.0001, respectively; n.s. denotes no significant difference (analyzed using Prism ver. 7). Confocal microscopic BODIPY and DIC images of HEK 293 cells treated with (B) BODIPY-9P2-2 or (C) 9P2-2-BODIPY with each unlabeled peptide at a total concentration of 5 μM (labeled : unlabeled = 1:4 molar ratio). The arrows and arrowheads mean cells in which fluorescently labeled peptides accumulated on the membrane surface and cells that are undergoing blebbing, respectively. Scale bar, 50 μm.

A

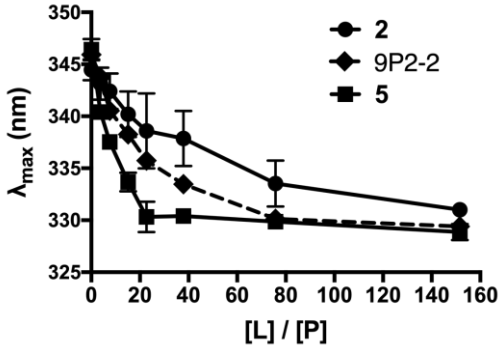

B

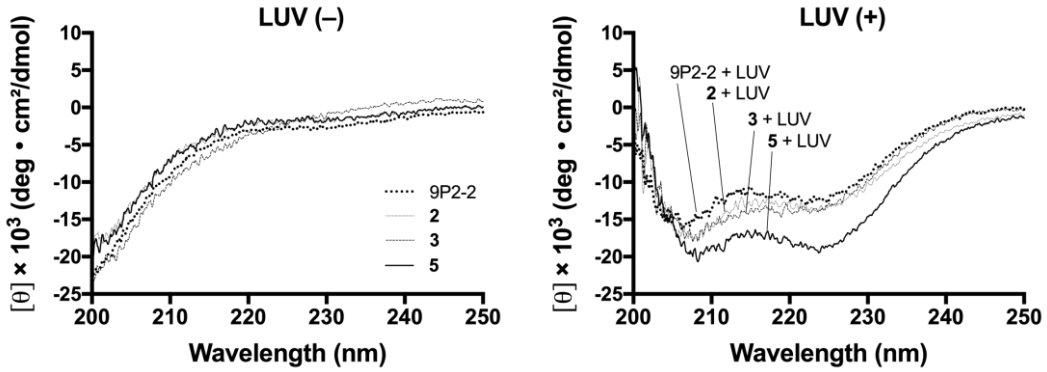

C

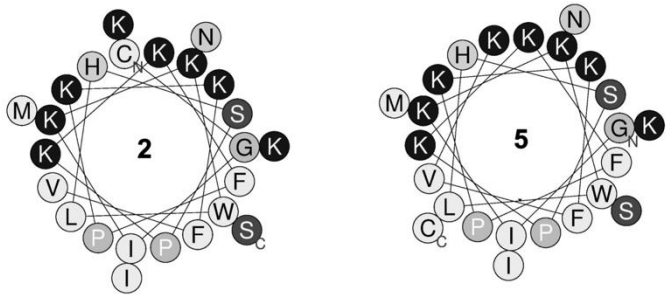

Figure 4 (A) Binding of 9P2-2 (diamonds), **2** (circles), and **5** (squares) to POPC/POPG (1:1) LUVs. Peptide solutions (4 μM) were titrated with POPC/POPG (1:1) LUVs at 30 ºC. Fluorescence spectra of the Trp residue were recorded at an excitation wavelength of 280 nm. The wavelength of maximal

intensity is plotted as a function of the [L]/[P] ratio. (B) CD spectra of the peptides (20 μM) in the absence (LUV (–)) or presence (LUV (+)) of 2 mM POPC/POPG (1:1) LUVs at 30 ºC. (C) Helical wheels of **2** and **5** using Heliquest (https://heliquest.ipmc.cnrs.fr).

For Table of Contents Use Only

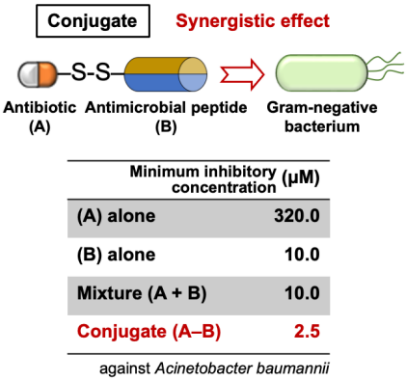

	Minimum inhibitory concentration (μM)
(A) alone	320.0
(B) alone	10.0
Mixture (A + B)	10.0
Conjugate (A–B)	2.5

against *Acinetobacter baumannii*

Development of antimicrobial peptide-antibiotic conjugates to improve the outer membrane permeability of antibiotics against Gram-negative bacteria

Ruka Yamauchi, Kenichi Kawano, Yousuke Yamaoka, Aoi Taniguchi, Yoshiaki Yano, Kiyosei Takasu, and Katsumi Matsuzaki

Antimicrobial peptide–antibiotic conjugates via a disulfide bond markedly exhibited high antibacterial activities against Gram-negative bacteria by improving the outer membrane permeability of antibiotics.

Supporting Information

Development of antimicrobial peptide-antibiotic conjugates to improve the outer membrane permeability of antibiotics against Gram-negative bacteria

Ruka Yamauchi[a, #], Kenichi Kawano[a, #], Yousuke Yamaoka[a], Aoi Taniguchi[a], Yoshiaki Yano[a,b], Kiyosei Takasu[a], and Katsumi Matsuzaki[a, *]

a) Graduate School of Pharmaceutical Sciences, Kyoto University, 46-29 Yoshida-Shimoadachi-cho, Sakyo-ku, Kyoto 606-8501, Japan

b) School of Pharmacy and Pharmaceutical Sciences, Mukogawa Women's University, 11-68 Koshien Kyuban-cho, Nishinomiya, Hyogo 663-8179, Japan

[#] These authors equally contributed.

*) Author to whom correspondence should be addressed.

E-mail: mkatsumi@pharm.kyoto-u.ac.jp

Table of Contents

Supporting Figures and Table

Supporting Figures

Figure S1

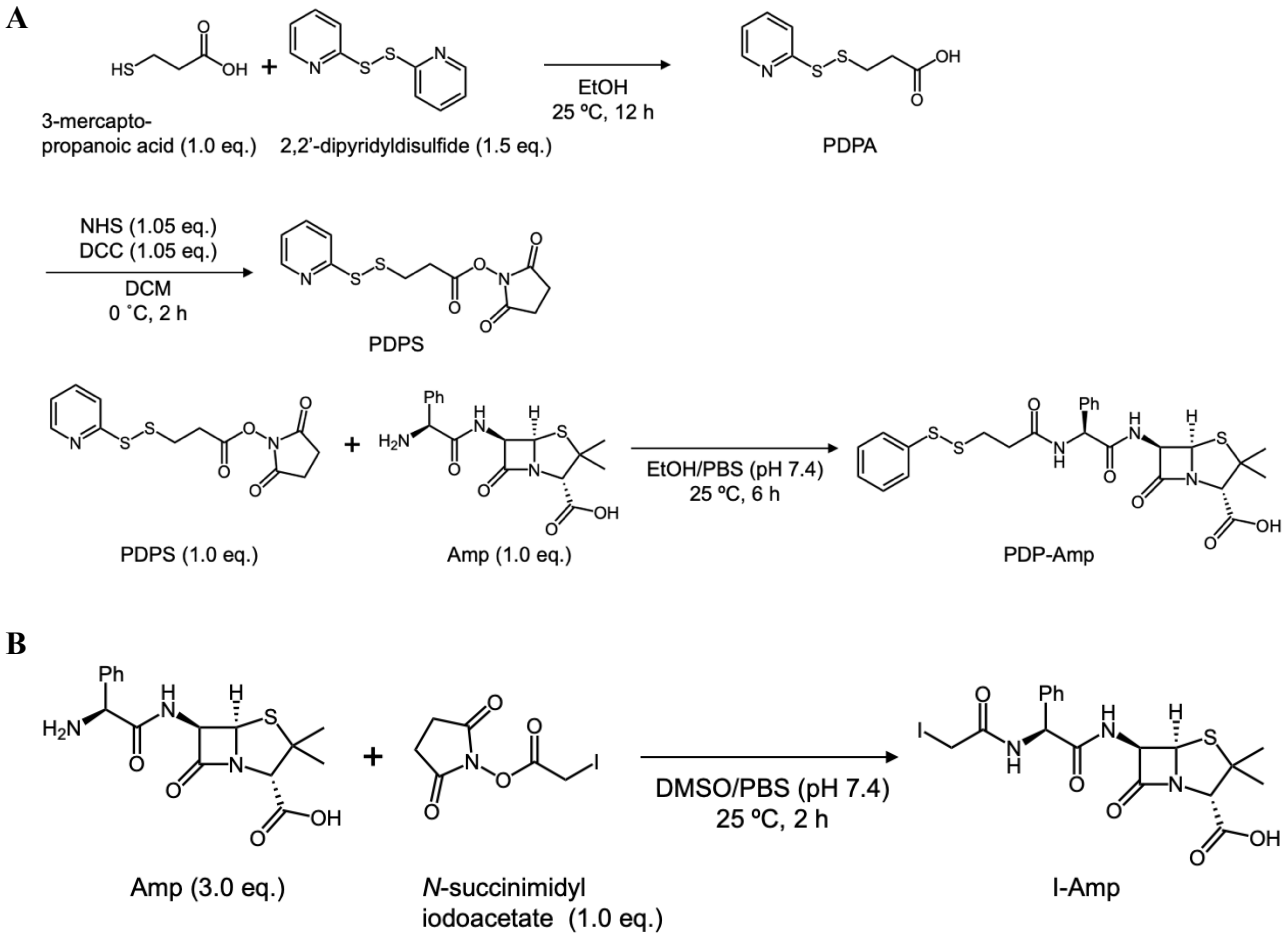

Figure S1 The synthesis scheme of thiol group-reactive Amp derivates. (A) PDP-Amp and (B) I-Amp.

Table S1 The purity verification and MS analysis of the compounds.

Compound	Theoretical $[M + H]^+$	Observed (*m/z*)	Purity
Cys-9P2-2 (**2**)	2871.7	2873.0	>95%
9P2-2-Cys (**5**)	2871.7	2872.2	>95%
Cys-oncocin (**8**)	2492.4	2492.3	>95%
oncocin-Cys (**10**)	2492.4	2492.6	>95%
Amp-SS-9P2-2 (**3**)	3306.8	3308.4	>95%
9P2-2-SS-Amp (**6**)	3306.8	3308.9	>95%
Amp-SS-oncocin (**9**)	2927.5	2927.1	>95%
oncocin-SS-Amp (**11**)	2927.5	2927.3	>95%
Amp-S-9P2-2 (**4**)	3260.8	3263.2	>95%
9P2-2-S-Amp (**7**)	3260.8	3263.7	>85%
BODIPY-9P2-2	3286.9	3288.2	>95%
9P2-2-BODIPY	3286.9	3288.5	>95%

Figure S2

Cys-9P2-2 (**2**)

A

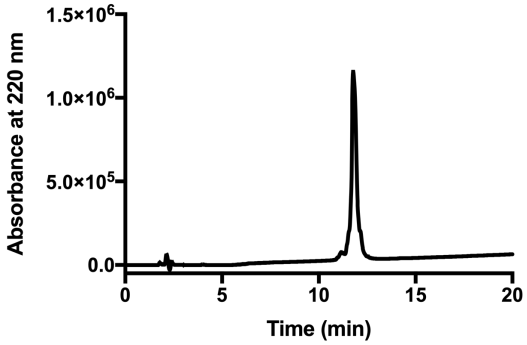

B

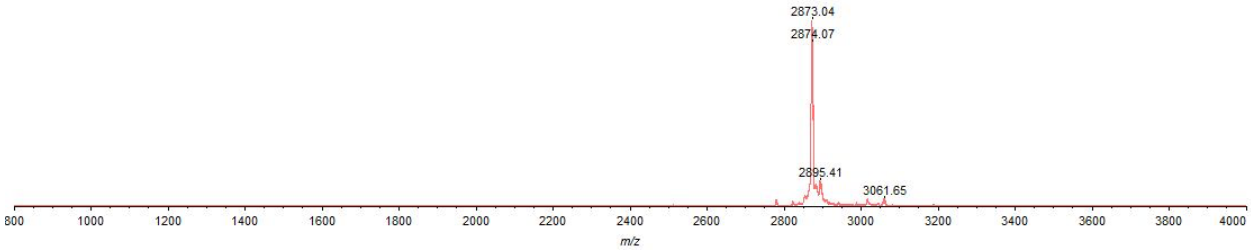

Figure S2. HPLC profile and MALDI-MS analysis of Cys-9P2-2.

The HPLC profile (A) and the MALDI-MS analytical data (B) of the purified peptide. (A) The purity and the retention time were analyzed by RP-HPLC on a COSMOSIL 5C_{18}-AR-II column (4.6 mm I.D. × 150 mm) using a linear gradient from 10 to 90% acetonitrile in 0.1% aqueous TFA (detection at 220 nm) at 40 ºC. The purity of the peptide was calculated to be over 95% based on the peak area. (B) Calculated $[M + H]^+$ = 2871.7, observed *m/z* = 2873.0

Figure S3

9P2-2-Cys (**5**)

A

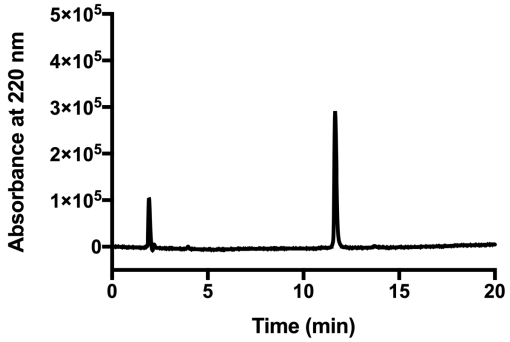

B

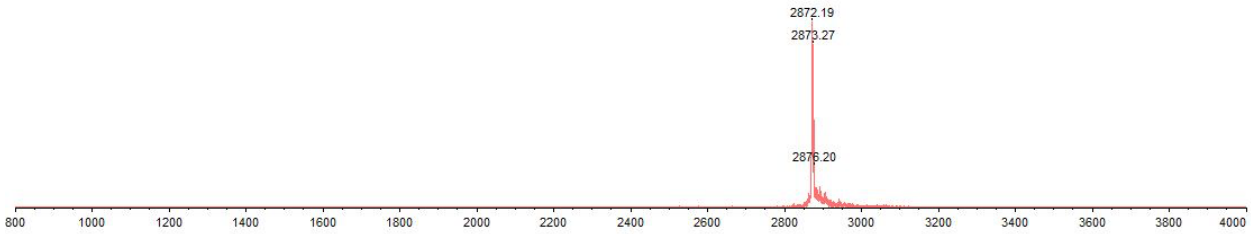

Figure S3. HPLC profile and MALDI-MS analysis of 9P2-2-Cys.

The HPLC profile (A) and the MALDI-MS analytical data (B) of the purified peptide. (A) The purity and the retention time were analyzed by RP-HPLC on a COSMOSIL 5C_{18}-AR-II column (4.6 mm I.D. × 150 mm) using a linear gradient from 10 to 90% acetonitrile in 0.1% aqueous TFA (detection at 220 nm) at 40 ºC. The purity of the peptide was calculated to be over 95% based on the peak area. (B) Calculated $[M + H]^+$ = 2871.7, observed *m/z* = 2872.2

Figure S4

Cys-oncocin (**8**)

A

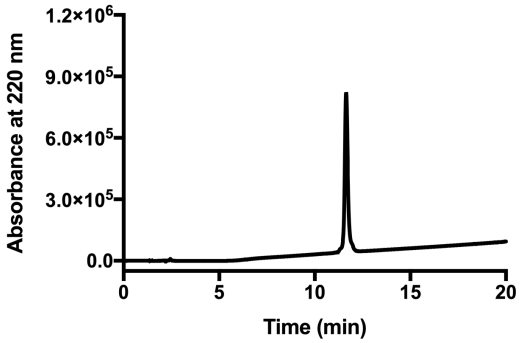

B

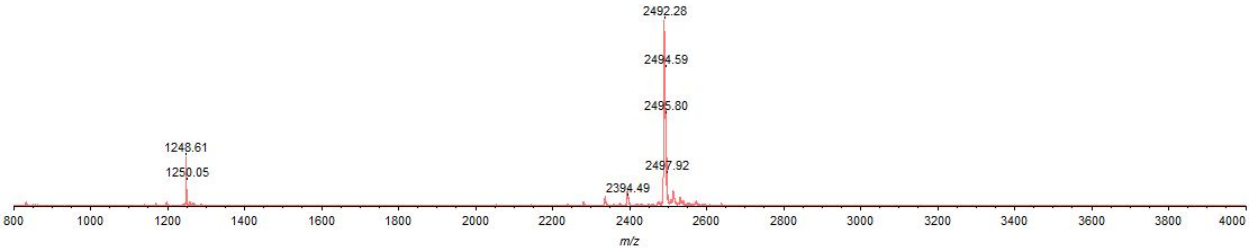

Figure S4. HPLC profile and MALDI-MS analysis of Cys-oncocin.

The HPLC profile (A) and the MALDI-MS analytical data (B) of the purified peptide. (A) The purity and the retention time were analyzed by RP-HPLC on a COSMOSIL $5C_{18}$-AR-II column (4.6 mm I.D. × 150 mm) using a linear gradient from 10 to 90% acetonitrile in 0.1% aqueous TFA (detection at 220 nm) at 40 ºC. The purity of the peptide was calculated to be over 95% based on the peak area. (B) Calculated $[M + H]^+ = 2492.4$, observed *m/z* = 2492.3

Figure S5

oncocin-Cys (**10**)

A

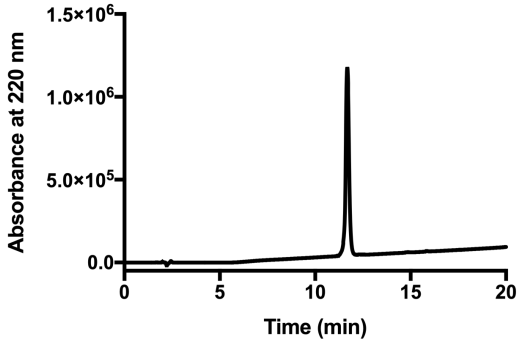

B

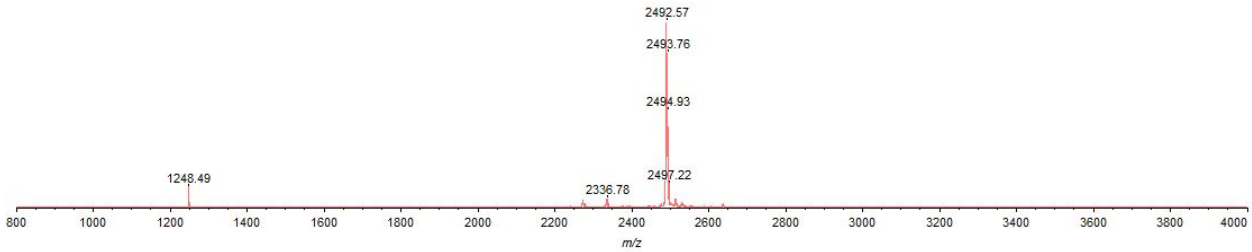

Figure S5. HPLC profile and MALDI-MS analysis of oncocin-Cys.

The HPLC profile (A) and the MALDI-MS analytical data (B) of the purified peptide. (A) The purity and the retention time were analyzed by RP-HPLC on a COSMOSIL $5C_{18}$-AR-II column (4.6 mm I.D. × 150 mm) using a linear gradient from 10 to 90% acetonitrile in 0.1% aqueous TFA (detection at 220 nm) at 40 ºC. The purity of the peptide was calculated to be over 95% based on the peak area. (B) Calculated $[M + H]^+ = 2492.4$, observed $m/z = 2492.6$

Figure S6

Amp-SS-9P2-2 (**3**)

A

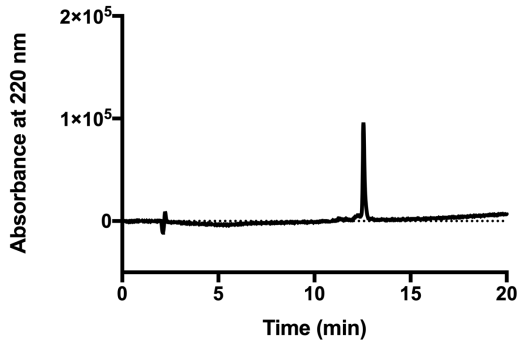

B

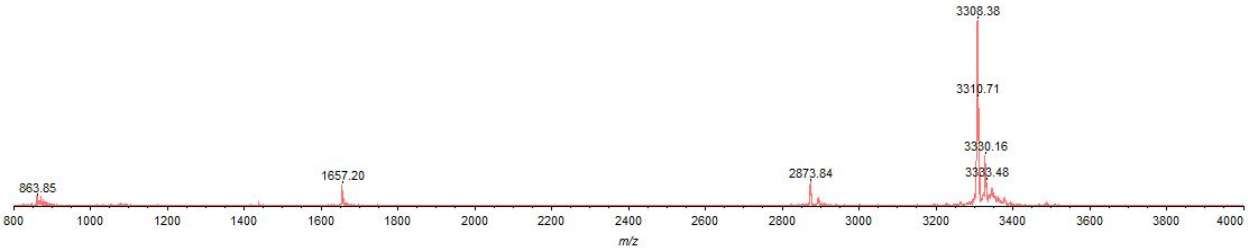

Figure S6. HPLC profile and MALDI-MS analysis of Amp-SS-9P2-2.

The HPLC profile (A) and the MALDI-MS analytical data (B) of the purified peptide. (A) The purity and the retention time were analyzed by RP-HPLC on a COSMOSIL 5C_{18}-AR-II column (4.6 mm I.D. × 150 mm) using a linear gradient from 10 to 90% acetonitrile in 0.1% aqueous TFA (detection at 220 nm) at 40 ºC. The purity of the peptide was calculated to be over 95% based on the peak area. (B) Calculated $[M + H]^+$ = 3306.8, observed *m/z* = 3308.4

Figure S7

9P2-2-SS-Amp (**6**)

A

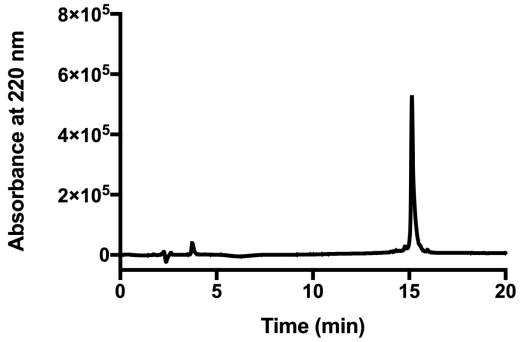

B

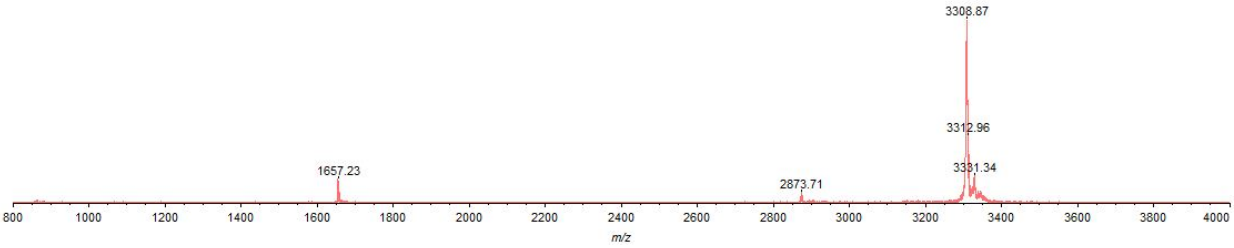

Figure S7. HPLC profile and MALDI-MS analysis of 9P2-2-SS-Amp.

The HPLC profile (A) and the MALDI-MS analytical data (B) of the purified peptide. (A) The purity and the retention time were analyzed by RP-HPLC on a COSMOSIL $5C_{18}$-AR-II column (4.6 mm I.D. × 150 mm) using a linear gradient from 10 to 90% acetonitrile in 0.1% aqueous TFA (detection at 220 nm) at 40 ºC. The purity of the peptide was calculated to be over 95% based on the peak area. (B) Calculated $[M + H]^+$ = 3306.8, observed *m/z* = 3308.9

Figure S8

Amp-SS-oncocin (**9**)

A

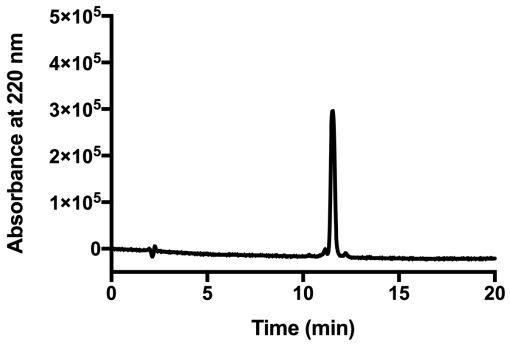

B

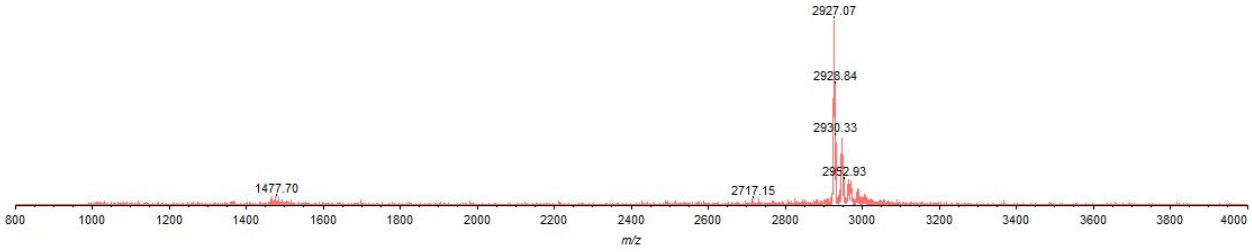

Figure S8. HPLC profile and MALDI-MS analysis of Amp-SS-oncocin.

The HPLC profile (A) and the MALDI-MS analytical data (B) of the purified peptide. (A) The purity and the retention time were analyzed by RP-HPLC on a COSMOSIL 5C_{18}-AR-II column (4.6 mm I.D. × 150 mm) using a linear gradient from 10 to 90% acetonitrile in 0.1% aqueous TFA (detection at 220 nm) at 40 ºC. The purity of the peptide was calculated to be over 95% based on the peak area. (B) Calculated $[M + H]^+$ = 2927.5, observed *m/z* = 2927.1

Figure S9

oncocin-SS-Amp (**11**)

A

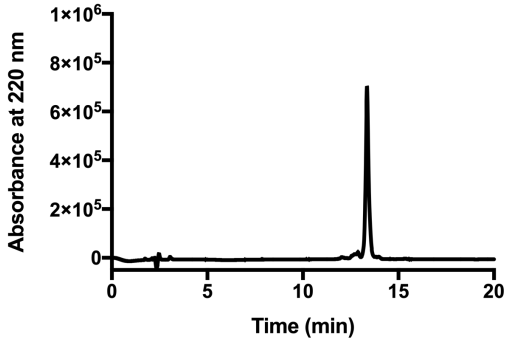

B

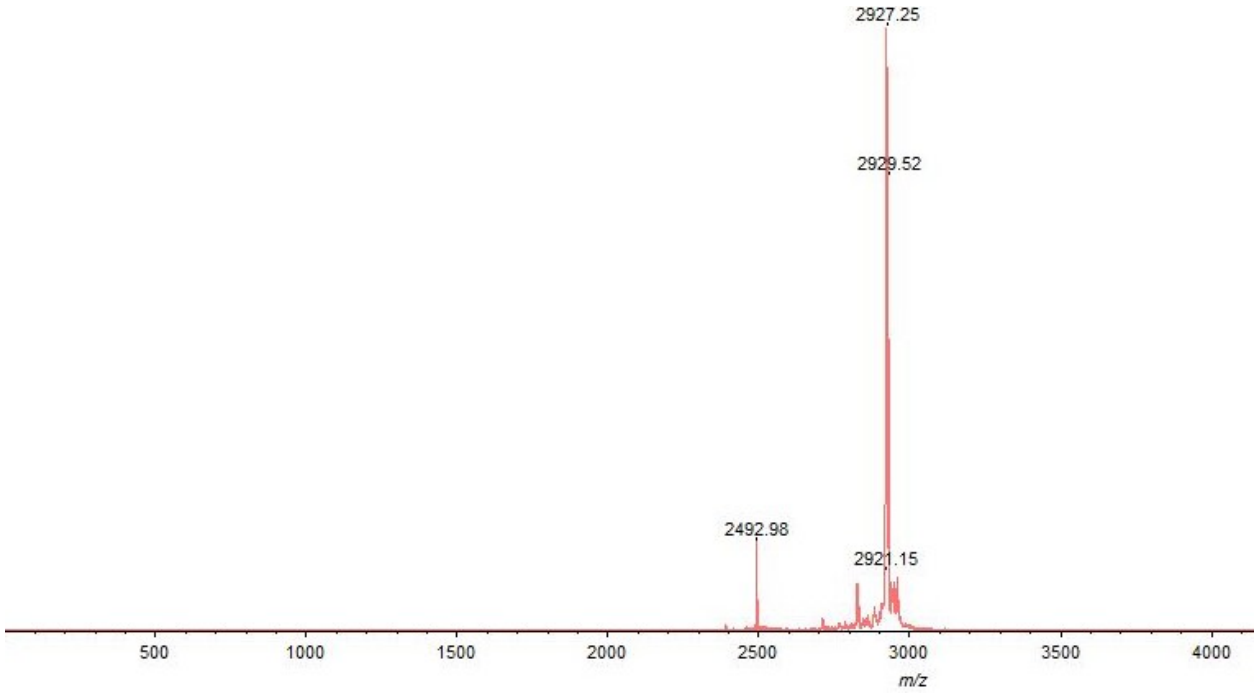

Figure S9. HPLC profile and MALDI-MS analysis of oncocin-SS-Amp.

The HPLC profile (A) and the MALDI-MS analytical data (B) of the purified peptide. (A) The purity and the retention time were analyzed by RP-HPLC on a COSMOSIL $5C_{18}$-AR-II column (4.6 mm I.D. × 150 mm) using a linear gradient from 10 to 90% acetonitrile in 0.1% aqueous TFA (detection at 220 nm) at 40 ºC. The purity of the peptide was calculated to be over 95% based on the peak area. (B) Calculated $[M + H]^+ = 2927.5$, observed $m/z = 2927.3$

Figure S10

Amp-S-9P2-2 (**4**)

A

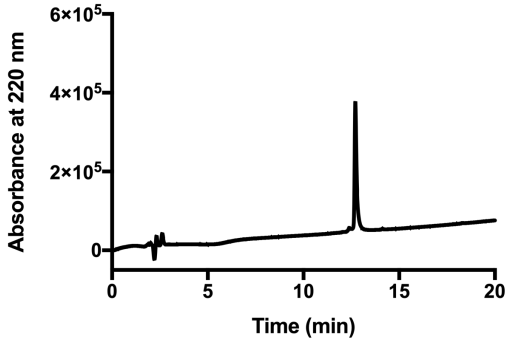

B

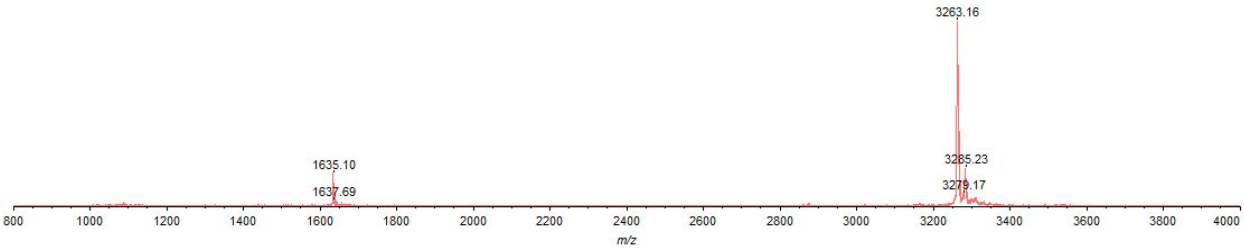

Figure S10. HPLC profile and MALDI-MS analysis of Amp-S-9P2-2.

The HPLC profile (A) and the MALDI-MS analytical data (B) of the purified peptide. (A) The purity and the retention time were analyzed by RP-HPLC on a COSMOSIL 5C_{18}-AR-II column (4.6 mm I.D. × 150 mm) using a linear gradient from 10 to 90% acetonitrile in 0.1% aqueous TFA (detection at 220 nm) at 40 ºC. The purity of the peptide was calculated to be over 95% based on the peak area. (B) Calculated $[M + H]^+$ = 3260.8, observed *m/z* = 3263.2

Figure S11

9P2-2-S-Amp (**7**)

A

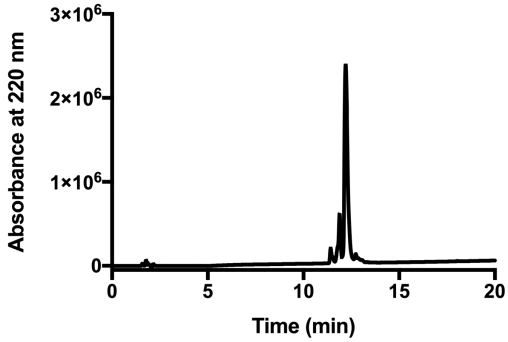

B

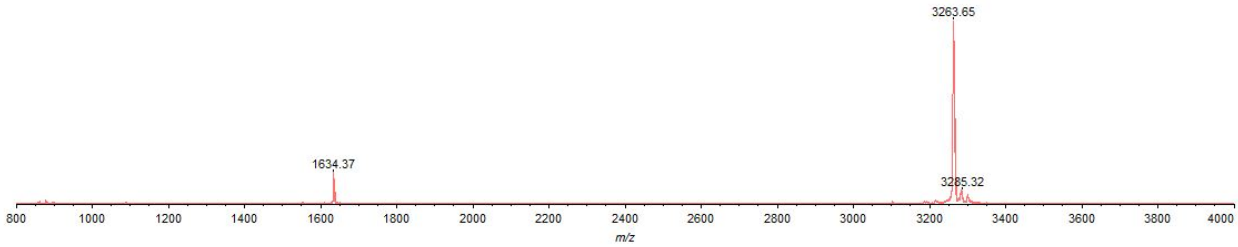

Figure S11. HPLC profile and MALDI-MS analysis of 9P2-2-S-Amp.

The HPLC profile (A) and the MALDI-MS analytical data (B) of the purified peptide. (A) The purity and the retention time were analyzed by RP-HPLC on a COSMOSIL $5C_{18}$-AR-II column (4.6 mm I.D. × 150 mm) using a linear gradient from 10 to 90% acetonitrile in 0.1% aqueous TFA (detection at 220 nm) at 40 ºC. The purity of the peptide was calculated to be over 85% based on the peak area. (B) Calculated $[M + H]^+ = 3260.8$, observed $m/z = 3263.7$

Figure S12

BODIPY-9P2-2

A

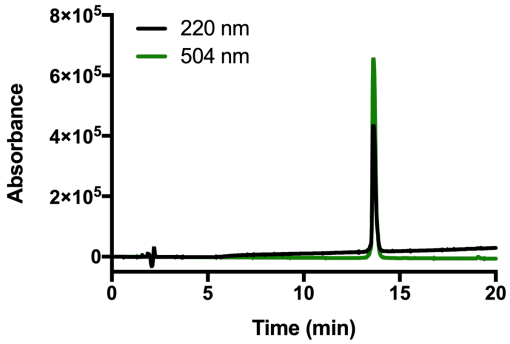

B

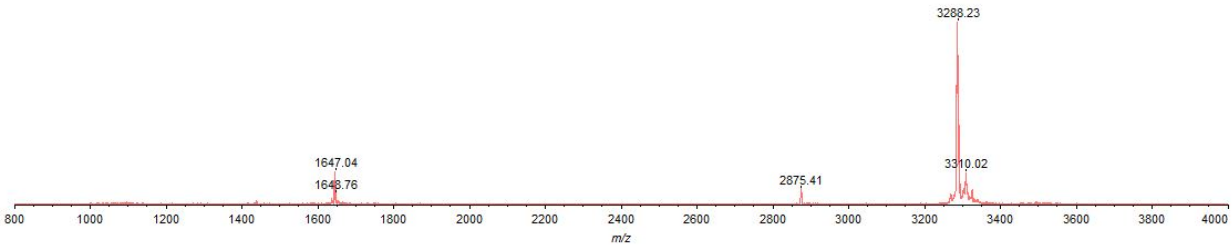

Figure S12. HPLC profile and MALDI-MS analysis of BODIPY-9P2-2.

The HPLC profile (A) and the MALDI-MS analytical data (B) of the purified peptide. (A) The purity and the retention time were analyzed by RP-HPLC on a COSMOSIL $5C_{18}$-AR-II column (4.6 mm I.D. × 150 mm) using a linear gradient from 10 to 90% acetonitrile in 0.1% aqueous TFA (detection at 220 and 504 nm) at 40 ºC. The purity of the peptide was calculated to be over 95% based on the peak area. (B) Calculated $[M + H]^+ = 3286.9$, observed $m/z = 3288.2$

Figure S13

9P2-2-BODIPY

A

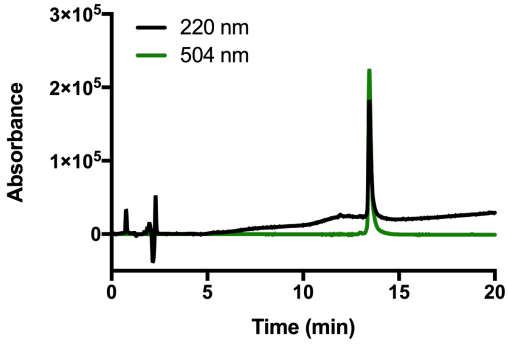

B

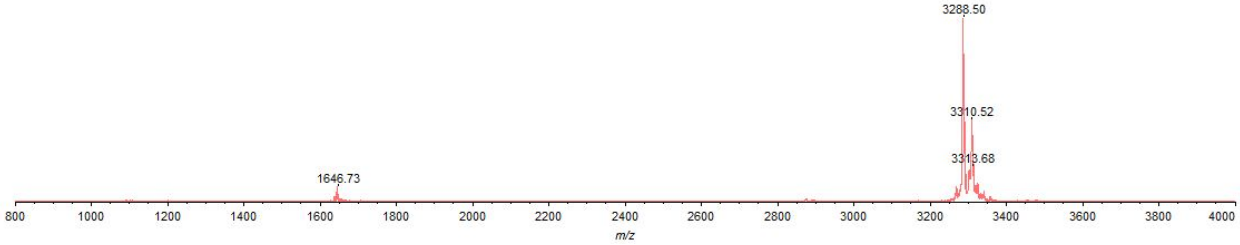

Figure S13. HPLC profile and MALDI-MS analysis of 9P2-2-BODIPY.

The HPLC profile (A) and the MALDI-MS analytical data (B) of the purified peptide. (A) The purity and the retention time were analyzed by RP-HPLC on a COSMOSIL 5C_{18}-AR-II column (4.6 mm I.D. × 150 mm) using a linear gradient from 10 to 90% acetonitrile in 0.1% aqueous TFA (detection at 220 and 504 nm) at 40 ºC. The purity of the peptide was calculated to be over 95% based on the peak area. (B) Calculated $[M + H]^+$ = 3286.9, observed *m/z* = 3288.5

Figure S14

A BODIPY-9P2-2 (*E. coli*)

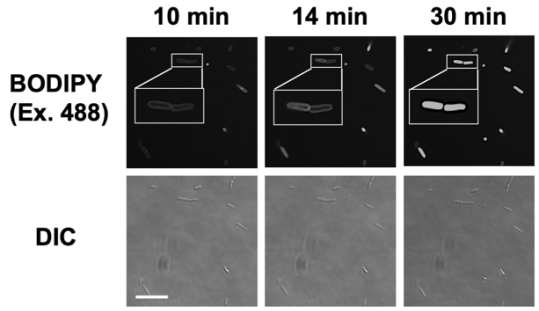

B 9P2-2-BODIPY (*E. coli*)

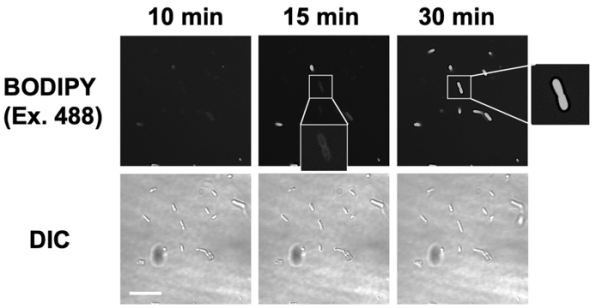

Figure S14 Confocal microscopic images of *E. coli* treated with BODIPY labeled 9P2-2 peptides. (A) BODIPY-9P2-2 or (B) 9P2-2-BODIPY with each unlabeled peptide at 5 μM (labeled : unlabeled = 1:4 molar ratio). Upper and lower figures are BODIPY fluorescence images excited at 488 nm and DIC images, respectively. Scale bar, 10 μm.

Figure S15

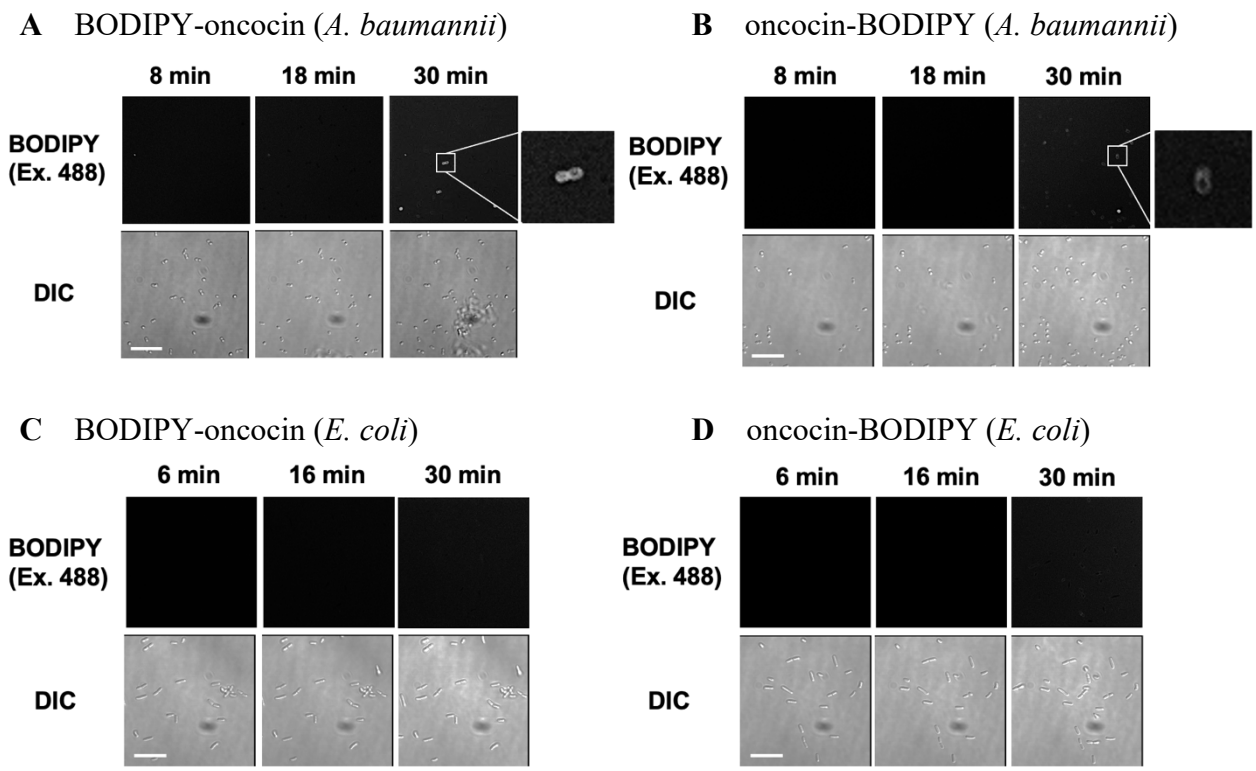

Figure S15 Confocal microscopic images of *A. baumannii* and *E. coli* treated with BODIPY labeled oncocin peptides. *A. baumannii* treated with (A) BODIPY-oncocin or (B) oncocin-BODIPY with each unlabeled peptide at a concentration of 40 μM (labeled : unlabeled = 1:39 molar ratio), respectively. *E. coli* treated with (C) BODIPY-oncocin or (D) oncocin-BODIPY with each unlabeled peptide at a concentration of 40 μM (labeled : unlabeled = 1:39 molar ratio), respectively. Upper and lower figures are BODIPY fluorescence images excited at 488 nm and DIC images, respectively. Scale bar, 10 μm.

Figure S16

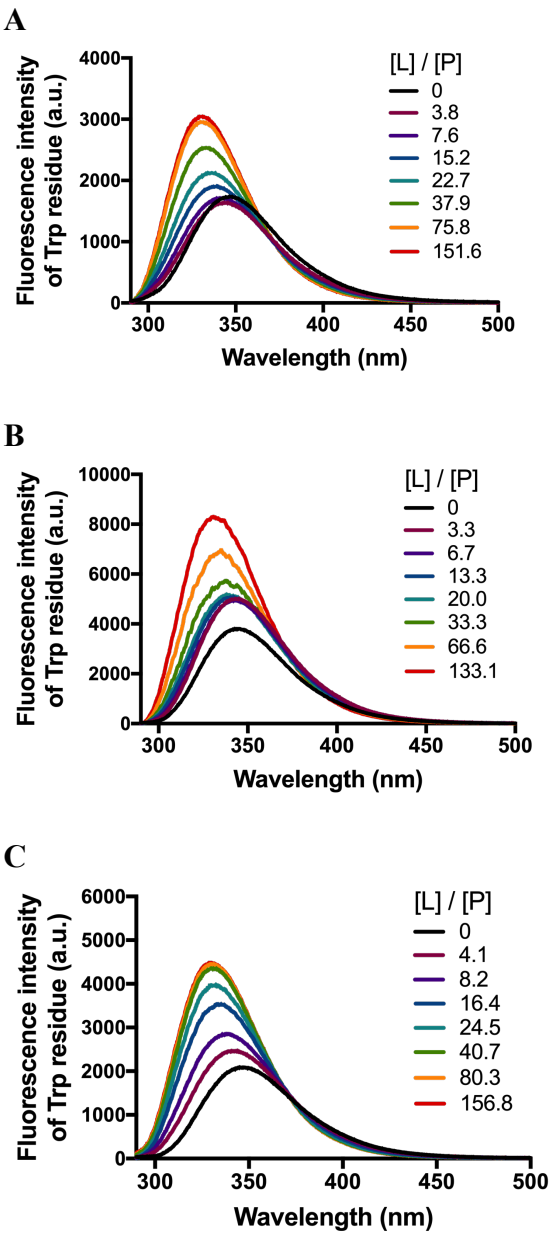

Figure S16 The peak shift of Trp fluorescence depending on the [L]/[P] ratio. The fluorescence spectra of (A) 9P2-2, (B) **2**, and (C) **5** (4 μM) were recorded at an excitation wavelength of 280 nm while being titrated with LUVs at various concentrations.